LOW POWER ORC-ORC SYSTEMS FOR HEAT PUMP APPLICATIONS

J. Demierre, Researcher, D. Favrat, Professor;
Ecole Polytechnique Fédérale de Lausanne, LENI-IGM-STI, Station 9, CH1015 Lausanne, Switzerland;

Abstract: This paper presents a study of a residential (about 20kW) ORC-ORC (Organic Rankine Cycle) thermally driven heat pump. The system works with three different temperature levels similar to absorption heat pumps. The proposed concept is a hermetic system using the same working fluid in both ORC's with a radial compressor and turbine on a single high-speed shaft. The use of gas bearings enables the system to be oil-free. This gives the system the advantage of low maintenance costs.
Using the same working fluid in both cycles does not come without difficulty due to the large difference between the high and low temperature levels. Depending on the application, the temperature difference in the heat exchanger at the heat source might be substantial which results in large exergy losses. Nevertheless preliminary calculations show that COP's higher than 1.6 could be expected which would be competitive with absorption heat pump alternatives.

Key Words: *thermally driven heat pumps*, *oil-free, high speed refrigerant vapor bearings, Organic Rankine Cycles*

1 INTRODUCTION

Single combustion in boilers is a very inefficient way of heating. The higher cost of fuels and pollution concerns are likely to put more and more political pressure to prevent the use of boilers for most heating purposes. Alternatives are all linked to heat pumps allowing the value the renewable heat from the environment. Thermally driven heat pumps from a variety of fuels including wood pellets or natural gas are usually realized using an absorption heat pump or by a combination of heat engine cycle with a compression heat pump cycle or a combination of both. One concept of the second category has been proposed by Strong (Strong, 1980) and is based on the use of an ORC engine cycle driving a reversed ORC heat pump cycle, both using the same fluid. Such a concept can be made using scroll expander and compressor usually lubricated with oil or by an oil-free high speed dynamic compressor-expander assembly rotating on refrigerant vapour bearings. Unfortunately earlier attempts of the latter failed because of lack of appropriate materials and of the problematic of the CFC refrigerants, which were, at the time, among the best candidates for high temperature cycles. Progress in materials and in finding new fluids, to substitute the CFCs with a reasonably high temperature chemical stability and/or acceptance, allow the reconsideration of this approach with HFC-134a or R600 as key working fluid candidates. One concept of miniature high speed centrifugal compressor directly driven by a high speed electric motor (Schiffmann, 2006) rotating on refrigerant gas bearings opens the way to such devices with or without electric motor.

2 ORC-ORC HIGH SPEED CONCEPT

An ORC-ORC system is composed of an ORC engine cycle and a reversed Rankine heat pump cycle (Figure 1). The condenser (and the subcooler if introduced) is common to both cycles. The power from the ORC turbine is used to drive the compressor of the heat pump cycle. This system works between three main temperature levels and is therefore similar to an absorption heat pump. Heat is provided at high temperature (by a boiler for example) at the supercritical evaporator of the topping ORC and at low (geothermal probe) temperature at the evaporator of the heat pump ORC. Heat is supplied to the house heating system by the unit condenser at medium temperature.

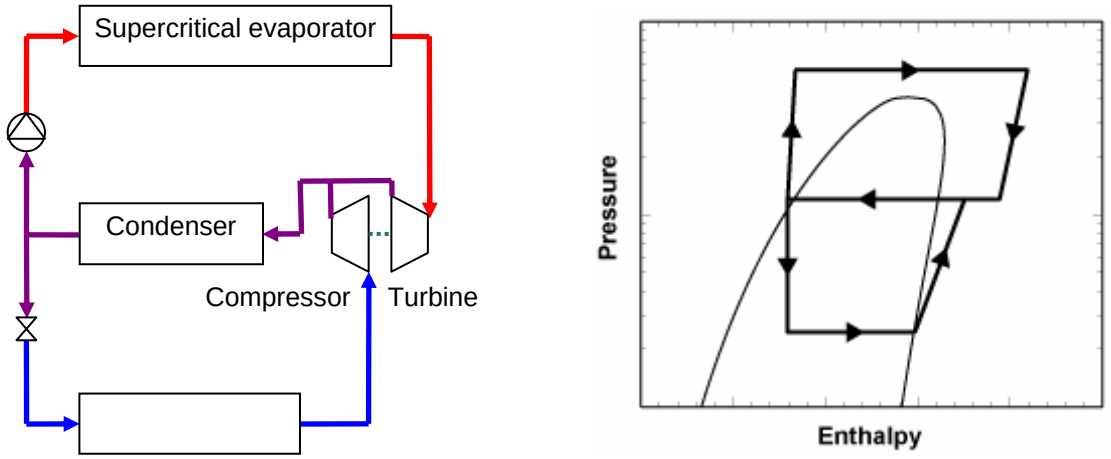

Figure 1: Schematic flowsheet and Log P –h diagram of a simple ORC-ORC heat pump unit

The studied concept is a low power system (about 20 kW heat at the condenser in the case treated here) with one-stage radial compressor and turbine. The compressor and turbine are directly coupled on the same shaft rotating on refrigerant gas bearings. This gives the system the advantage of being oil-free, fully hermetic and with low maintenance costs in spite of the more complex circuitry. Because of the characteristics of dynamic compressors and turbines a low density fluid is preferred and refrigerant HFC-134a has been selected at this stage. It is chemically stable at relatively high temperatures (at least up to 180°C).

3 ORC-ORC MODEL AND OPTIMIZATION TOOL

3.1 ORC-ORC Model

An ORC-ORC model has been developed using a commercial flowsheeting and process software, Vali-Belsim. The flowsheet is shown in Figure 2. The R134a thermodynamic property model from REFPROP is used. At first pressure drops in the heat exchangers and pipes, and heat losses are neglected. The expansion in the valve is considered to be isenthalpic. The pump isentropic efficiency is considered to be constant and equal to 0.5. The losses related to the compressor-turbine shaft are neglected. A polynomial approximation of the correlation of Rohlik (1968) is used to model the turbine isentropic efficiency η_T. This relation gives the maximum efficiency that can be achieved for a fixed turbine specific speed n_{sT}.

$$n_{sT} = \frac{\omega \dot{V}_T^{1/2}}{\Delta h_{0sT}^{3/4}}$$

with $\dot{V}_T$: the volumetric flow at the turbine outlet
ω : the angular velocity
Δh_{0sT} : the isentropic enthalpy difference between the inlet and outlet of the turbine

The used polynomial function is

$$\eta_T = -12.427\, n_{sT}^{\,6} + 54.081\, n_{sT}^{\,5} - 93.44\, n_{sT}^{\,4} + 81.408\, n_{sT}^{\,3} - 38.101\, n_{sT}^{\,2} + 9.3522\, n_{sT} - 0.1306 \ .$$

The compressor isentropic efficiency η_C is modeled following a similar method. A correlation (adapted from Balje 1981) that relates the maximum efficiency to the compressor specific speed n_{sC} is approximated. The compressor specific speed is defined by:

$$n_{sC} = \frac{\omega\, \dot{V}_C^{\,1/2}}{\Delta h_{0sC}^{\,3/4}}$$

with $\dot{V}_C$: the volumetric flow at the compressor inlet
ω : the angular velocity
Δh_{0sC} : the isentropic enthalpy difference between the outlet and inlet of the compressor

The approximation is based only on the curve that corresponds to radial compressors. The resulting polynomial function is

$$\eta_C = -0.0663\, n_{sC}^{\,6} + 0.6165\, n_{sC}^{\,5} - 2.3356\, n_{sC}^{\,4} + 4.6343\, n_{sC}^{\,3} - 5.143\, n_{sC}^{\,2} + 3.0398\, n_{sC} + 0.1242 \ .$$

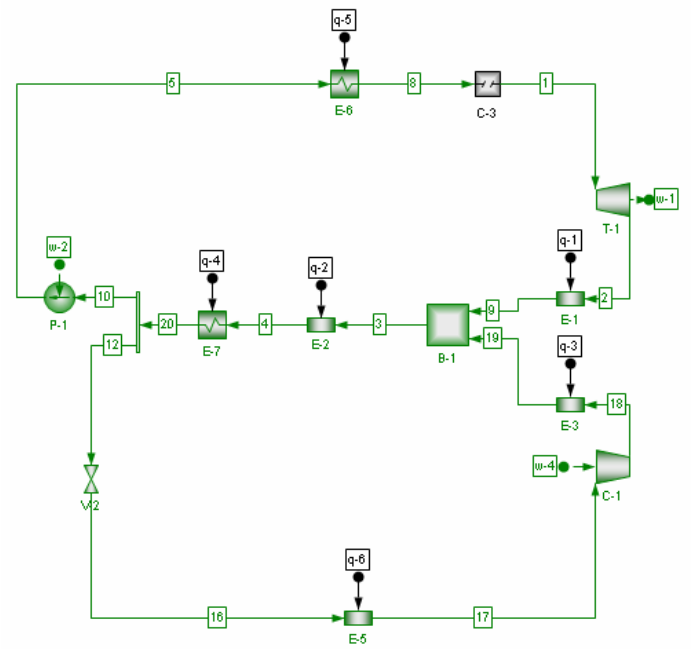

- In this decomposition the compressor work w-4 and the expander work w-1 are separated even though in the concept w-1=w-4.
- w-2 is the work (electricity) supplied to the pump by the grid.
- q-6 and q-5 are mainly the contributions from respectively the cold source and the combustion gases.

Figure 2: ORC-ORC model flowsheet on Vali-Belsim

In order to estimate the turbine size that optimizes the efficiency, the corresponding wheel peripherical speed U_{2T} is determined using the following relation:

$$U_{2T} / C_{sT} = 0.7 \qquad \text{with} \qquad C_{sT} = \sqrt{2\,\Delta h_{0sT}}$$

Then, the wheel diameter D_{2T} is given by

$$D_{2T} = 2\frac{U_{2T}}{\omega} \ .$$

The optimal size of compressor wheel is evaluated by determining the corresponding specific diameter:

$$d_{sC} = \frac{D_{2C}\ \Delta h_{0sC}{}^{1/4}}{\dot{V}_C{}^{1/2}} \qquad \text{with} \qquad D_{2C}: \text{the compressor wheel diameter.}$$

The optimal d_{sC} is estimated using the relation

$$n_{sC} \cdot d_{sC} = 3$$

which approximates the line of best efficiency on Balje's $n_s - d_s$ chart for the radial compressor zone. Then, the compressor wheel diameter D_{2C} is calculated by using the d_{sC} definition.

3.2 Utilities

Two heat sources are defined. The first one is the combustion gases resulting from a stoichiometric combustion of methane that cools down to a temperature as low as possible

(for example to 4°C in winter time of our calculations). Heat delivered by the condensation of the water from the combustion gases is also considered. The combustion and cooling are simulated using the software Vali-Belsim. The second heat source is the glycol water from a geothermal probe (that cools down from 4°C to 0°C in our calculations). The enthalpy variation is calculated with

$$\Delta h_{GW} = c_{GW} \cdot \Delta T \qquad \text{with} \qquad c_{GW} = 3.5 \frac{\text{kJ}}{\text{kg K}} \ .$$

The heat demands include domestic hot water and water for heating. Domestic water is assumed to be heated from 10°C to 60°C and the floor heating water is heated from 30°C to 35°C. The enthalpy variation is evaluated by

$$\Delta h_{W} = c_{W} \cdot \Delta T \qquad \text{with} \qquad c_{W} = 4.18 \frac{\text{kJ}}{\text{kg K}} \ .$$

Hot water production and heating represent respectively 23% and 77% of the heat demand.

3.3 Energy Integration

The utilities and the ORC-ORC streams are thermally integrated using an in-house energy integration computer tool, called “Easy” (Maréchal F. et al.1998). The streams of the whole system are shown in Figure 3. Each stream is associated with a differentiated $\Delta T_{min}/2$ value (Table 1). The values are used to determine, for two streams α and β, the minimum temperature difference $\Delta T_{min\,\alpha\beta}$ for which a heat exchange is possible:

$$\Delta T_{min\,\alpha\beta} = \left(\Delta T_{min}/2\right)_{\alpha} + \left(\Delta T_{min}/2\right)_{\beta}$$

Table 1: $\Delta T_{min}/2$ values for the streams of the system

Stream	Heating water Hot water	Glycol water	Fumes	ORC-ORC
$\Delta T_{min}/2$ [K]	2	2	5	2

The mass flows of the ORC-ORC are fixed and the ones of the utilities are computed in order to maximize the COP, which is defined by

$$COP = \frac{\dot{Q}_{W}^{-}}{\dot{Q}_{fumes}^{+} + \dfrac{\dot{E}_{p}^{+}}{0.56}} \ .$$

$\dot{Q}_{W}^{-}$ is the heat given to the water (hot water and heating), $\dot{Q}_{fumes}^{+}$ is the heat given by the fumes resulting from the methane combustion and $\dot{E}_{p}^{+}$ is the electrical power consumed by the ORC-ORC pump (which is the only electrical power consumed by the ORC-ORC). $\dot{E}_{p}^{+}$ is divided by 0.56 to take into account for the efficiency of a modern combined cycle power plant that produces this electrical power, in order to define a COP which is strictly based on the conversion of the fuel (here, methane) into heat. The exact expression for $\dot{Q}_{fumes}^{+}$ is

$$\dot{Q}^{+}_{fumes} = \dot{M}_F \left(\Delta h_i^0 + \hat{h}_F\right) + \dot{M}_A \hat{h}_A - \dot{M}_G \hat{h}_G + \dot{M}_{cond} h_{cond} \ ,$$

where $\dot{M}_F$, $\dot{M}_A$ and $\dot{M}_G$ are respectively the mass flow of the fuel (methane, in our calculations), the air and the fumes. Δh_i^0 is the lower heating value of the fuel (here, for the standard state, P^0 = 1.01325 bar and T^0 = 25°C). $\hat{h}_F$ and $\hat{h}_A$ are respectively the physical enthalpy difference (compared to the standard state) of the fuel and the air at boiler inlet. $\hat{h}_G$ is the physical enthalpy difference of the fumes at boiler exhaust. $\dot{M}_{cond}$ is the mass flow of the condensing water (produced during the combustion) and h_{cond} is the water latent heat. At first approximation, $\dot{Q}^{+}_{fumes}$ will be simplified as:

$$\dot{Q}^{+}_{fumes} \cong \dot{M}_F \ \Delta h_i^0 \ .$$

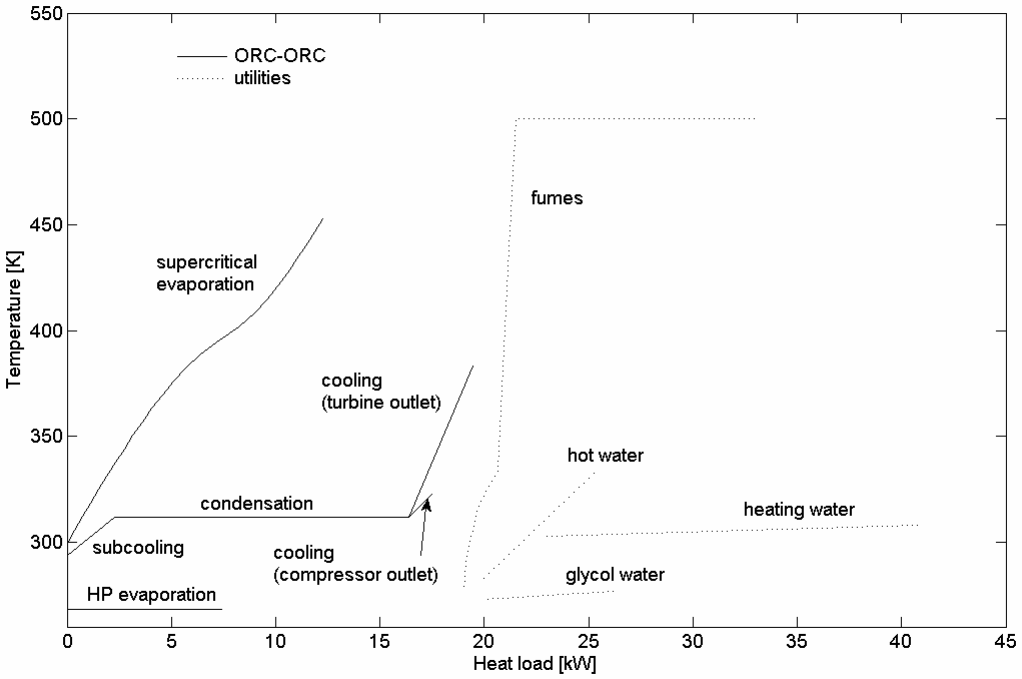

Figure 3: Streams of the system

3.4 Optimization

An in-house multiobjective optimization tool, MOO, which is based on a genetic algorithm, is used to generate optimal solutions. The optimization variables are listed below:

- N : the rotational speed of the turbine-compressor rotor
- P_{max} : the supercritical evaporation pressure
- T_{max} : the turbine inlet temperature
- P_{cond} : the condensation pressure
- ΔT_c : the subcooling temperature difference

An in-house software, Osmose, enables the communication between the different pieces of software (Vali-Belsim, Easy and MOO).

4 RESULTS

4.1 COP and Rotational Speed Optimization

A two-objective optimization is done with the COP maximization as first objective and the compressor-turbine rotational speed minimization as second objective. The optimization variables lower and upper bounds are given below:

- N [rpm] : $[0.5 \cdot 10^5 \;\; 6 \cdot 10^5]$
- P_{max} [bar] : [41 80]
- T_{max} [K] : [373 453]
- P_{cond} [bar] : [7 15]
- ΔT_c [K] : [-35 0]

The pareto curve resulting from this computation is shown on Figure 4. The points correspond to optimal solutions which are tradeoffs between minimum rotational speed and maximum COP. Two points were not eliminated by the algorithm, however they are clearly not optimal. It appears that the COP increases with the rotational speed because the efficiency of the compressor-turbine unit improves. The COP reaches a maximum value for a rotational speed beyond 430'000 rpm but the windage and bearings friction losses are not yet considered. The conception of a compressor-turbine unit for such a speed is hardly feasible, moreover the COP improvement for values higher than 250'000 rpm is negligible. Table 2 gives the turbine and compressor wheel diameter for a point with a rotational speed of about 200'000 rpm.

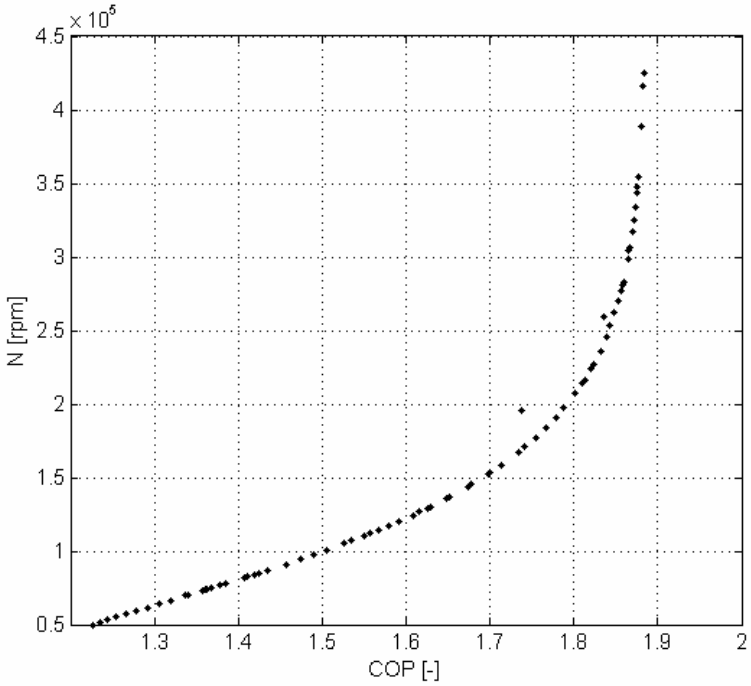

Figure 4: Pareto curve of the optimization with the COP and rotational speed as objectives

Table 2: COP and turbine and compressor wheel diameter for a design with a rotational speed N = 207557 rpm

COP	D_{2T}	D_{2C}
[-]	[mm]	[mm]
1.8017	20.3	23.6

Figure 5 shows the supercritical evaporation pressure P_{max} as a function of the rotational speed. It appears that the optimal pressure is lower than 80 bar, the upper bound, and depends strongly on N below 200'000 rpm. In fact, there is a tradeoff between maximum pressure to maximize the ORC theoretical efficiency and optimal pressure ratio regarding the turbine efficiency. The optimal pressure ratio depends on N.

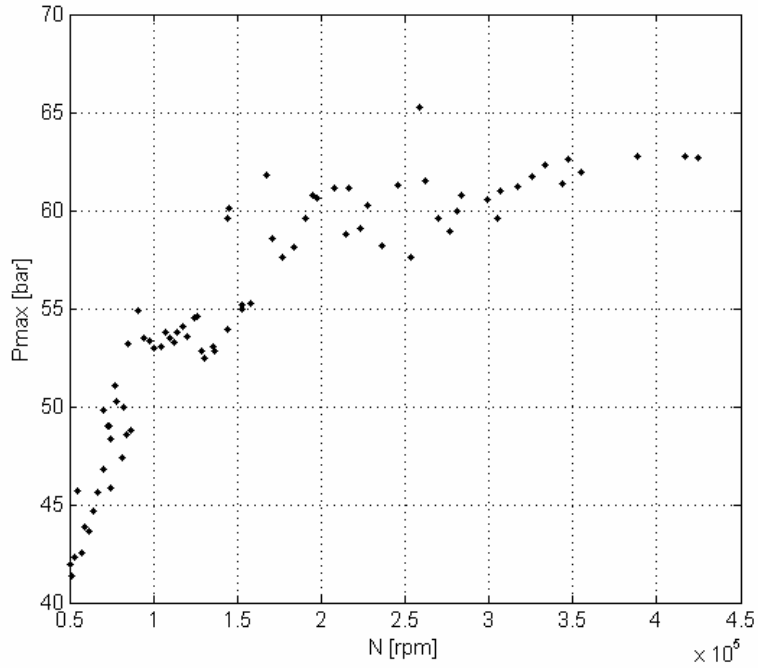

Figure 5: N vs. P_{max} for the optimization with the COP and rotational speed as objectives

4.2 Sensibility analysis to turbine inlet temperature

To analyze the sensibility of the COP to the turbine inlet temperature T_{max}, a two-objective optimization is done with the COP maximization as first objective and the T_{max} minimization as second objective. The optimization variables lower and upper bounds are listed below:

- N [rpm] : $[0.5 \cdot 10^5 \;\; 2.5 \cdot 10^5]$
- P_{max} [bar] : [41 80]
- T_{max} [K] : [373 493]
- P_{cond} [bar] : [7 15]
- ΔT_c [K] : [-35 0]

The pareto curve of this computation is given on Figure 6 and, as expected, shows that the COP improves with increasing T_{max}. This highlights the importance to work with a fluid that can be used at a temperature as high as possible. It also shows that good COP values (~1.5) can be reached at relatively low temperature (~100°C). This means that heat sources at temperature as low as 120°C can be exploited with this system and this application (floor heating and geothermal brine source).

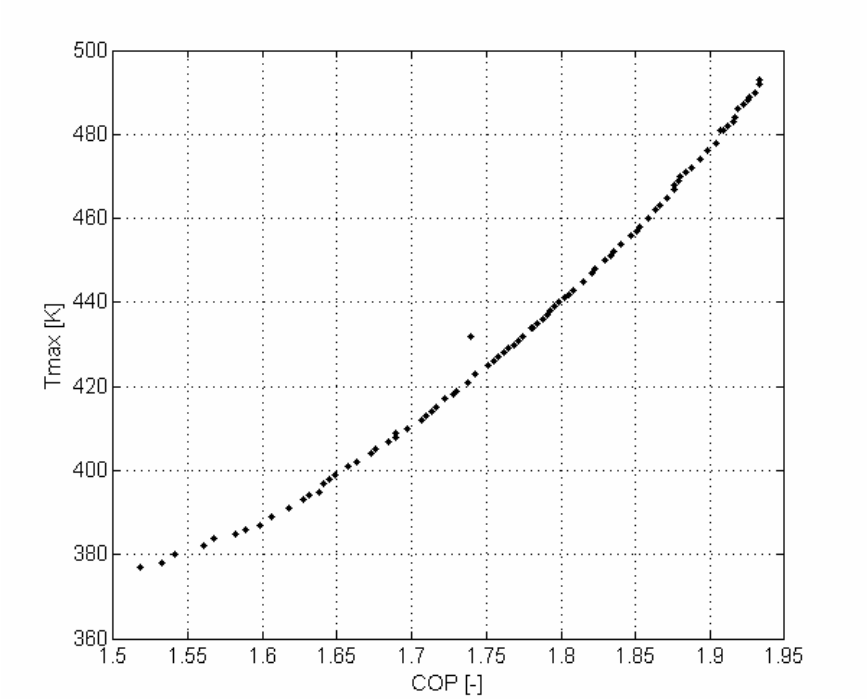

Figure 6: Pareto curve of the optimization with the COP and turbine inlet temperature as objectives

4.3 Simplified System

The same optimization as shown in section 4.1 is done but with no heat exchange possible between the fumes and the water, and between the ORC streams themselves. The resulting pareto curve and the one presented in section 4.1 are shown on Figure 7. It appears that the optimal solutions of the computation with the restricted heat exchangers are only a few percent worse regarding the COP. The composite curves of equivalent solutions from the two optimizations are given on Figure 8. The corresponding flow diagrams are shown on Figure 9. The heat exchange between the fumes and the heat pump cycle evaporation is eliminated because it represents a small amount of power and moreover it has no effect on the COP. However, for future concepts of air source heat pumps, the use of the end part of the fumes cooling will be considered, with interesting possibilities to assist defrosting.

5 PERSPECTIVE

Based on the first approach the next step will be the introduction of the friction losses (windage and bearings) and the detailed design of turbine and compressor. For the latter a particular design is already under testing. Additional studies will include a separate high speed oil-free pump for the engine ORC, multi-stage units to address the market of boiler substitution as well as the feasibility of a topping cogeneration cycle.

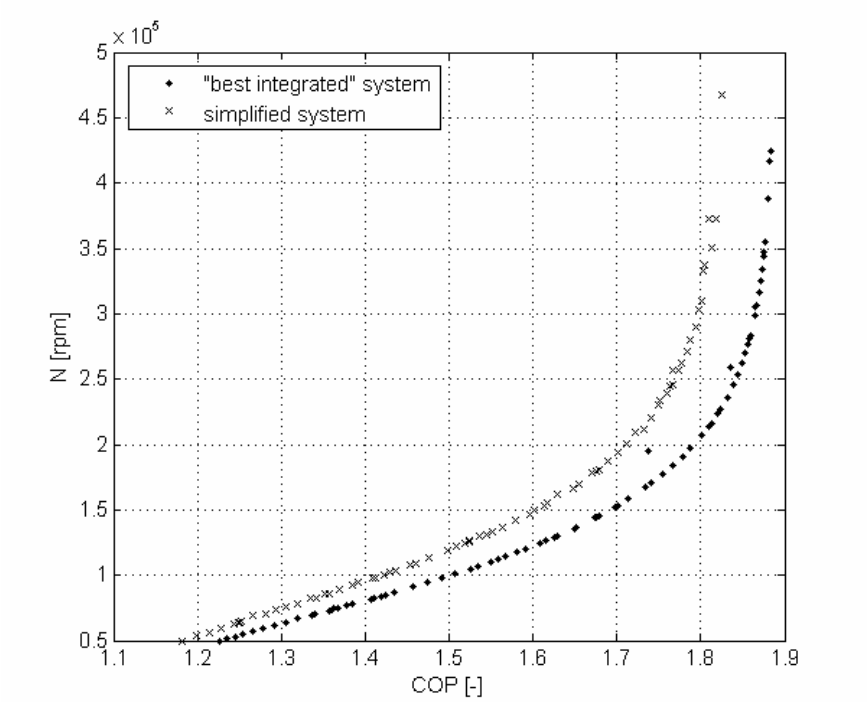

Figure 7: Pareto curves comparison of the "best integrated" system and simplified system

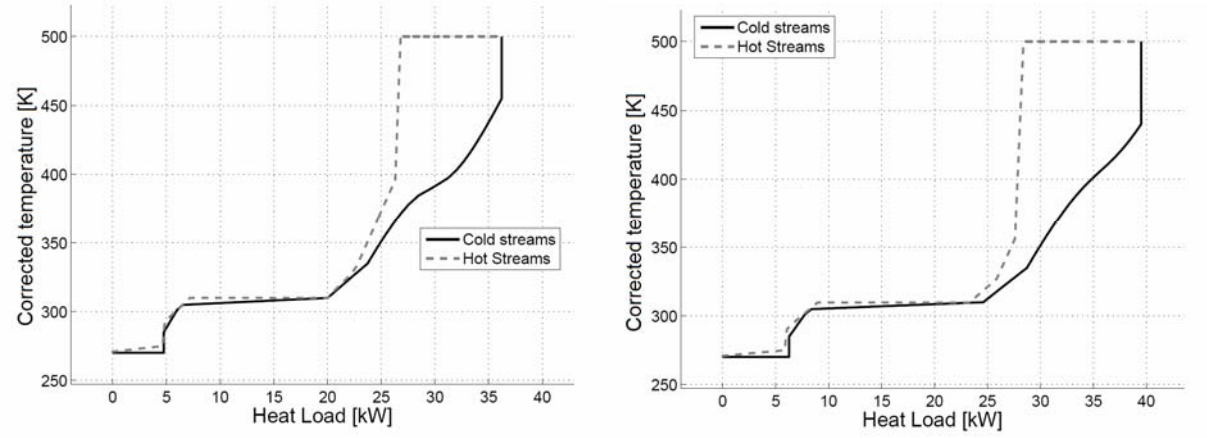

Figure 8: Composite curves of the "best integrated" system and simplified system (corrected temperature is equal to $T + (\Delta T_{min} / 2)$ for cold streams and to $T - (\Delta T_{min} / 2)$ for hot streams).

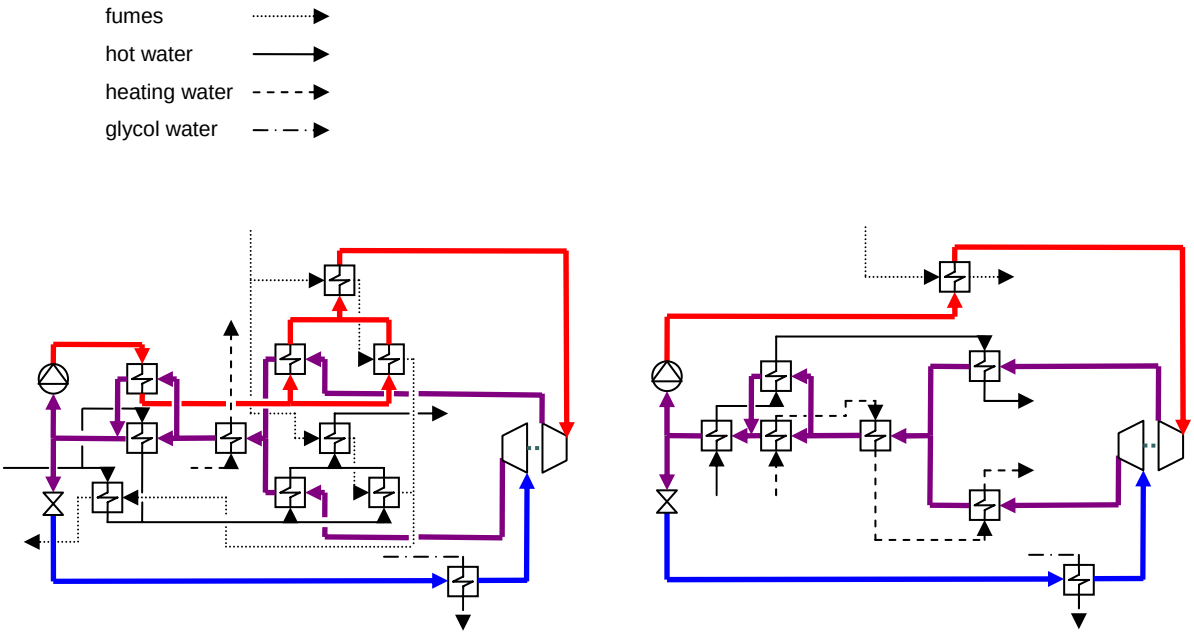

Figure 9: Flow diagrams of the "best integrated" system and simplified system

6 CONCLUSION

An ORC-ORC model with a high speed compressor-turbine unit has been developed. The model enables the estimation of the compressor and turbine optimal size and rotational speed. An energy integration software and a multiobjective optimization tool are used to generate optimal designs. A two-objective optimization on the COP and the compressor-turbine rotational speed is done and highlights the trade-off that exists between those two variables. Sensibility of the COP to the turbine inlet temperature is studied. The importance regarding the COP to use a working fluid that can work at high temperature is shown. A comparison between the "best system" from the energy integration point of view and a simpler system is done. The results show that great COP's can be obtained with low power ORC-ORC systems and efficient high speed compressor-turbine units for those applications seem to be feasible.

7 REFERENCES

Strong D.T.G. 1980. "Development of a directly fired domestic heat pump," PhD thesis, University of Oxford.

Schiffmann J., Favrat D. 2006. "High speed low power radial turbocompressor for oil-free heat pumps," *Compressor Engineering Conference*, Purdue.

Belsim, 2006. Vali IV. http://www.belsim.com.

Lemmon E., McLinden M., Huber M. 2002. "NIST Reference Fluid Thermodynamic and Transport Properties - REFPROP, Version 7.0," National Institute of Standards and Technology.

Balje O.E. 1981. "Turbomachines : A Guide to Design, Selection and Theory," New York, John Wiley & Sons.

Whitfield A., Baines N.C. 1990. “Design of Radial Turbomachines,” Essex, Longman Scientific & Technical.

Leyland G.B. 2002. “Multi-objective optimisation applied to industrial energy problems,” PhD thesis, Ecole polytechnique fédérale de Lausanne.

Maréchal F., Kalitventzeff B. 1998. “Process integration: Selection of the optimal utility system,” *Computers and chemical engineering 22*, S149–S156.

Molyneaux A. 2002. “A practical evolutionary method for the multi-objective optimisation of complex integrated energy systems including vehicle drivetrains,” PhD thesis, Ecole polytechnique fédérale de Lausanne.

Girardin L., Dubuis M., Darbellay N., Marechal F., Favrat D. 2008. “ENERGIS : A geographical information based system for the evaluation of integrated energy conversion systems in urban areas,” *21st International Conference on Efficiency, Cost, Optimization, Simulation and Environmental Impact of Energy Systems*, Krakow.

Gassner M., Maréchal F. 2007. “Methodology for the optimal thermo-economic, multi-objective design of thermochemical fuel production from biomass,” *submitted to: Computers and chemical engineering*.